

Melting and Solid-Solid Transition Temperatures at High Pressures for NH_4SCN , RbSCN , TlSCN , and CsSCN

William KLEMENT Jr.*

National Physical Research Laboratory, C.S.I.R., P.O. Box 395, Pretoria, South Africa

with an **Appendix—Lattice parameters of NH_4SCN and RbSCN at high temperatures**

by C. W. F. T. PISTORIUS†

(Received March 16, 1976)

Differential thermal analyses at high pressures have yielded the following trajectories for melting and solid-solid transitions in the several thiocyanates: (substance, transition, 1-bar transition temperature in $^{\circ}\text{C}$, initial slope (dT/dp) in deg kbar^{-1} , initial curvature ($-d^2T/dp^2$) in deg kbar^{-2} , approximate maximum pressure in kbar) NH_4SCN , melting, ≈ 146 , ~ 20 (tentative), —, ~ 3.5 ; NH_4SCN , (upper) solid-solid, 120 ± 4 , 12.6 ± 1.5 , —, 7.5 ; RbSCN , melting, 184 ± 2 , 15.7 ± 0.3 , 0.32 ± 0.05 , 36; RbSCN , solid-solid, 166 ± 3 , 13.5 ± 1.0 , 0.3 ± 0.1 , 30; TlSCN , melting, ≥ 234 , ≥ 10 (tentative) > 0 , 34; TlSCN , solid-solid, 99 ± 2 , 9.6 ± 1.0 , ≈ 0.17 , 34; CsSCN , melting, ≥ 206 , $\approx 14 \pm 1.5$, ~ 0.2 – 0.4 , 33; CsSCN , solid-solid, ≥ 197 , $\approx 11.8 \pm 1.0$, ~ 0.2 , 33. The solid-solid transitions investigated here for NH_4SCN , RbSCN and TlSCN appear to be closely-related, structurally, to the well-investigated transition in KSCN . The thermodynamics of the KSCN transition at 1-bar is discussed anew so as to be consistent with high pressure data. The transitions in these other thiocyanates are probably thermodynamically similar to the KSCN transition but the necessary data to establish the similarities are lacking. Lattice parameters for NH_4SCN and RbSCN show rapid variations with temperature below the solid-solid transition, as for KSCN . DSC and DTA results are presented for the 1-bar transition temperatures and entropy changes for NH_4SCN , RbSCN , TlSCN , CsSCN and also AgSCN . The entropy changes apparently associated with the structurally similar solid-solid transitions decrease with increasing cation polarizability.

Of the univalent thiocyanates, the phase relations¹⁾ in KSCN are, thus far, the most complex, with 5 polymorphs having been postulated up to ~ 44 kbar, although there is only one rather thoroughly investigated^{2,3)} solid-solid transition at 1-bar. NaSCN shows⁴⁾ only one polymorph to ~ 40 kbar, which differs in structure from the 1-bar KSCN polymorphs, as do the low temperature phase of NH_4SCN ,⁵⁾ the only known phase in AgSCN ⁶⁾ and the CsSCN ⁷⁾ phases. Besides data on the CsSCN phase relations at high pressures, this paper reports on the phase relations of NH_4SCN , RbSCN and TlSCN —all of which show phase transitions which apparently are similar to the KSCN transition. Also reported, in the Appendices, are a thermodynamic discussion of the KSCN transition more nearly in accord with existing data and lattice parameters for NH_4SCN and RbSCN at high temperatures.

Experimental

General Procedure. Transitions were detected by differential thermal analysis (DTA), using the piston-cylinder apparatus, furnace geometry and experimental procedures described previously.⁸⁾ Details of the runs for each substance are given below. After corrections for friction, pressures are believed accurate to ± 0.5 kbar. Temperatures, as measured with Chromel-Alumel thermocouples, are believed accurate to $\pm 2^{\circ}\text{C}$.

NH_4SCN . In both runs, Merck reagent grade material was contained in aluminium capsules, which had been treated with HNO_3 . The samples were dewatered by holding briefly above $\sim 100^{\circ}\text{C}$ before sufficient pressure had been applied to seal the capsules. The lower solid-solid transition, investigated by Bridgman,⁹⁾ was not studied. In the first

run, the upper solid-solid transition was observed by small but distinct breaks in the DTA signals, the corresponding temperatures agreeing to within $\pm 1^{\circ}\text{C}$ on heating and cooling. At least two heating/cooling cycles were run at each pressure to demonstrate reproducibility and, where possible, this is usual in all of these experiments. After increasing pressure ≥ 8 kbar, signals could not be reproduced satisfactorily and the black contents of the capsule indicated decomposition. No efforts were made to investigate the details of the decomposition. In the second run, the solid-

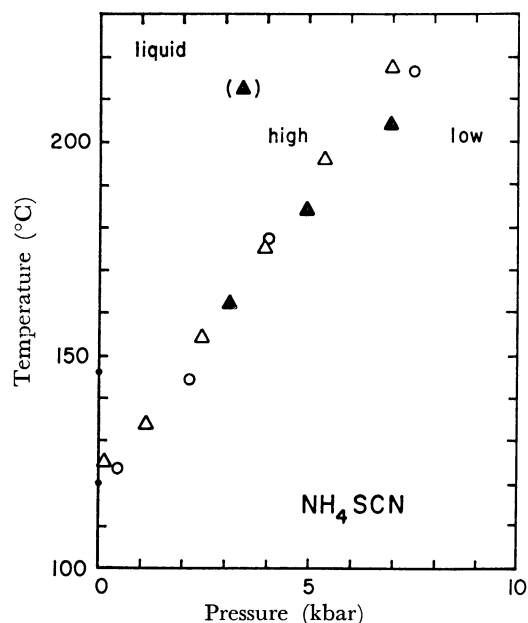


Fig. 1. Solid-solid and melting (point in parentheses and tentative) temperatures for NH_4SCN . Accepted 1-bar transition temperatures are indicated. Open symbols denote upstroke data; filled symbols denote downstroke data. Circles denote data from first run and triangles those from second run, both in aluminium capsules.

* On leave from School of Engineering and Applied Science, University of California, Los Angeles, California 90024, U.S.A.

† Deceased 12 XII 1975

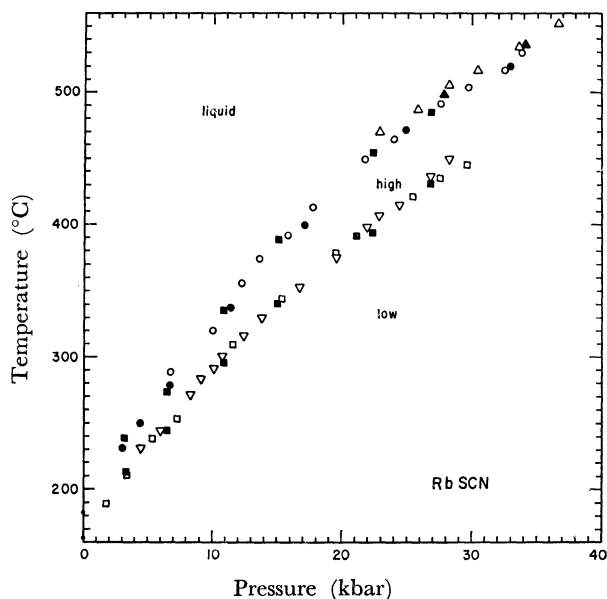


Fig. 2. Solid-solid and melting temperatures for RbSCN. Accepted 1-bar transition temperatures are indicated. Open symbols denote upstroke data; filled symbols denote downstroke data. Circles denote data from first run, triangles second and squares third run, all in aluminium capsules.

solid transition was observed as before and also data were obtained on decreasing pressure, which were used in the corrections for friction. A single datum was then obtained for the onset of melting, after which decomposition was indicated. The solid-solid transition data (Fig. 1) can be fitted by a straight line of slope $12.6 (\pm 10\%) \text{ deg kbar}^{-1}$ and intercept $120 \pm 4^\circ \text{C}$, which agrees with other 1-bar results.^{9,10} Taking the 1-bar melting point to be $\sim 146^\circ \text{C}$, the tentative slope for the melting curve is $\sim 20 \text{ deg kbar}^{-1}$ (Fig. 1).

RbSCN. In all three runs, aluminium capsules were used to contain the RbSCN, which was of unknown origin (and afterwards was shown by X-ray diffraction to contain some RbCl). In the first run, the melting curve was followed on both increasing and decreasing pressure, with the onset of the DTA signal taken for the melting temperature and undercoolings of ~ 5 to 25°C , roughly increasing with increasing temperature, observed for the freezing signals. In the second run, the solid-solid transition was detected as a small but distinct break in the DTA signal on heating and as a small peak on cooling, the temperatures corresponding to these features agreeing to within $2\text{--}3^\circ \text{C}$. Some corroborative melting data were also obtained in this run and the third run provided further corroborative data for both transitions. The data (Fig. 2) for the solid-solid transition can be fitted by a power series with 1-bar intercept $166 \pm 3^\circ \text{C}$, initial slope (dT/dp) $13.5 \pm 1.0 \text{ deg kbar}^{-1}$ and initial curvature $(-d^2T/dp^2)$ $0.3 \pm 0.1 \text{ deg kbar}^{-2}$. The melting data (Fig. 2) can be fitted by a power series with 1-bar intercept $184 \pm 2^\circ \text{C}$, initial slope $15.7 \pm 0.3 \text{ deg kbar}^{-1}$ and initial curvature $0.32 \pm 0.05 \text{ deg kbar}^{-2}$. Uncertainties are estimated by regression fits of individual sets of data and then of all the data taken together. It cannot be ruled out that the 'melting' curve here is actually the RbSCN-RbCl eutectic but neither the DTA signals nor the DSC results (below) indicated that the transition was spread out over a particularly large temperature range. Since RbCl melts at a much higher temperature than RbSCN and it is unlikely that there is much solid solubility of RbCl in RbSCN, the

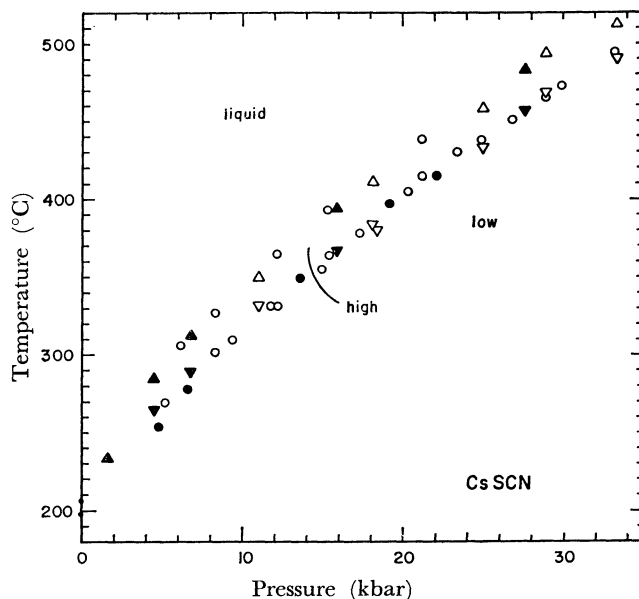


Fig. 3. Solid-solid and melting temperatures for CsSCN. Accepted 1-bar transition temperatures are indicated. Open symbols denote upstroke data; filled symbols denote downstroke data. Circles denote data from first run and triangles those from second run, both in aluminium capsules.

eutectic is probably 'degenerate', with composition and temperature very close to pure RbSCN and its true melting point, respectively. The present results (Fig. 2) for 'melting' are then a close lower bound to the melting of pure RbSCN.

CsSCN. In both runs, aluminium capsules were used to contain the material, which was obtained from K & K Laboratories. For the solid-solid transition, the onsets of the quite distinct DTA signals on heating and on cooling agreed to within $\pm 1^\circ \text{C}$ and were taken for the transition temperatures. The onset of the DTA signal on heating was taken as the melting temperature. In the first run, the DTA signals became so indistinct at the higher pressures that the run was abandoned without any data obtained on decrease of pressure. In the second run, however, data were quite reproducibly obtained on both increasing and decreasing pressure. Large undercoolings were observed after melting up to 50°C or 60°C — and the melt crystallized directly to the low-temperature phase since only the freezing signal was seen on cooling. The data (Fig. 3) for the solid-solid transition are not fitted well by the usual power series, with intercept $\approx 197^\circ \text{C}$, but there may be estimated an initial slope of $11.8 (\pm 1.0) \text{ deg kbar}^{-1}$ and an initial curvature $\sim 0.2 \text{ deg kbar}^{-2}$; similarly, for the melting data (Fig. 3) with intercept $\approx 206^\circ \text{C}$, there may be estimated an initial slope of $14 (\pm 1.5) \text{ deg kbar}^{-1}$ and an initial curvature $\sim 0.2\text{--}0.4 \text{ deg kbar}^{-2}$. The relatively poor fits afforded here by the power series to order p^2 may be due to the difficulties with the friction corrections at the lower pressures.

TlSCN. The first two runs were made with material from Electronic Space Products, in inconel and copper capsules, chronologically. No definite signals could be concluded for the solid-solid transition (see DSC results below) and only signals with rather indistinct onsets for melting; considerable undercooling was noted from the freezing signals. The next two runs were made with material from Ventron, in aluminium and then tantalum capsules. For the solid-solid transition, inflexions in the DTA signals on heating and distinct halts on cooling served to establish

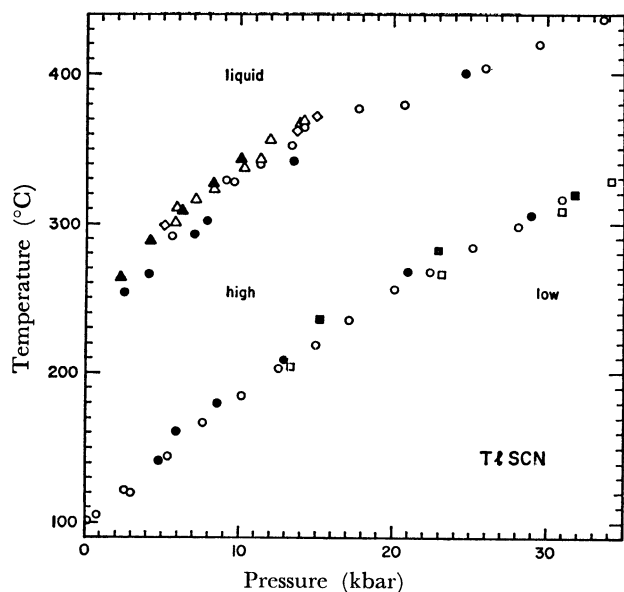


Fig. 4. Solid-solid and melting temperatures for TlSCN. Accepted 1-bar transition temperatures are indicated. Open symbols denote upstroke data; filled symbols denote downstroke data. Symbols for the several runs (capsule materials) are triangles—first (inconel); diamonds—second (copper); circles—third (aluminium); squares—fourth (tantalum). The melting data should be considered tentative.

the transition temperatures, which were the same, within experimental error, on heating and on cooling. The DTA signals for melting again showed only indistinct onsets and undercoolings were obvious from the freezing signals. The data (Fig. 4) for the solid-solid transition can be fitted by a power series with 1-bar intercept $99 \pm 2^\circ\text{C}$, initial slope $9.6 \pm 1.0 \text{ deg kbar}^{-1}$ and initial curvature $\approx 0.17 \text{ deg kbar}^{-2}$. The data (Fig. 4) for melting are disappointing, because of the poorly defined onsets (presumably due to impurities), and should only be considered as tentative. Only a poor fit is obtained with the usual power series but there may be estimated an initial slope $\geq 10 \text{ deg kbar}^{-1}$ and an initial curvature > 0 for a 1-bar intercept of $\sim 234^\circ\text{C}$.

AgSCN. One exploratory run was made with BDH Laboratory Reagent material contained in an aluminium capsule. Large DTA signals were observed $\leq 2 \text{ kbar}$, with poorly defined onsets near $\sim 180^\circ\text{C}$ on both heating and cooling. The run was abandoned after these signals disappeared and, subsequently, decomposition was indicated. No further work was attempted because of the lack of agreement with the DSC results (below).

DSC Results

Mr. S.J. Pretorius kindly made DSC runs on several substances. For NH_4SCN , the onset of the lower solid-solid transition was near 364 K, with a transition entropy of $\approx 2.2 \text{ cal mol}^{-1} \text{ deg}^{-1}$ (in good agreement with Bridgman⁹); the peak of the upper solid-solid transition was near 393 K, with a transition entropy $\geq 0.3 \text{ cal mol}^{-1} \text{ deg}^{-1}$; the onset of melting was near 419 K, with a melting entropy of $\approx 5.1 \text{ cal mol}^{-1} \text{ deg}^{-1}$; the latter temperatures agree satisfactorily with literature values.¹⁰

For RbSCN , one sample yielded the onset of melting near 455 K, with a melting entropy of $\approx 5.9 \text{ cal mol}^{-1} \text{ deg}^{-1}$, and the peak of the solid-solid transition near 436 K, with a transition entropy $\geq 0.6 \text{ cal mol}^{-1} \text{ deg}^{-1}$; another sample showed the same transition temperatures but somewhat smaller entropies, which are within the accuracy of the technique—say $\pm 10\%$; Wrzesnewsky¹⁰) apparently obtained a slightly higher melting temperature. For TlSCN, the material used initially showed the onset of melting near 498 K, with a melting entropy of $\approx 7.1 \text{ cal mol}^{-1} \text{ deg}^{-1}$, and only a poorly defined signal for the solid-solid transition; for the subsequent sample, the onset of melting was near 507 K, with a melting entropy of $\approx 7.7 \text{ cal mol}^{-1} \text{ deg}^{-1}$, and the peak of the solid-solid transition was near 372 K, with a transition entropy of $\geq 0.3 \text{ cal mol}^{-1} \text{ deg}^{-1}$; although the latter sample appears to be purer than the former, the onset of melting was not so sharp that impurities could be considered negligible. For AgSCN, a single run up from 330 K showed only what appeared to be melting, with onset near 534 K and the entropy $\approx 7.3 \text{ cal mol}^{-1} \text{ deg}^{-1}$; decomposition appeared to occur a few degrees higher. Mr. R. A. Pacey kindly made several DTA-DSC runs on the CsSCN used here—which essentially corroborated the previous results⁷) for transition temperatures and entropies.

Discussion

For melting, the Clausius-Clapeyron equation may be used to estimate the volume changes on fusion. With the absolute volume change in $\text{cm}^3 \text{ mol}^{-1}$ and the fractional volume change referred to the volume of the melting solid, there are estimated: for NH_4SCN , ~ 6.4 or $\sim 11\%$; for RbSCN , ~ 3.9 or $\approx 6.5\%$; for TlSCN, ≥ 3.2 or $\geq 6.1\%$; for CsSCN, ≈ 1.8 or $\approx 2.7\%$; also for KSCN, $6.0\text{--}7.1^{11}$ or $12.5 \pm 1\%$ and, for NaSCN, 4.3 ± 0.5^{12} or $\approx 9\%$. There appears to be a roughly linear correlation between the fractional volume change on fusion and the melting entropy for these compounds, the greatest deviations being for the least certain data (e.g., NH_4SCN and TlSCN). The NaSCN datum can be brought into better agreement with this correlation by subtracting an orientational entropy term from the melting entropy since the $(\text{SCN})^-$ ion is not disordered in the melting solid, as it presumably is for the other compounds. Such a correlation has not been discussed extensively for other sequences of chemically and structurally related compounds but then the present sequence offers a wider range of fractional volume changes and fusion entropies than is usually encountered for other sequences.

The solid-solid transition in CsSCN has an entropy change almost twice the melting entropy. The volume change for this transition is $\approx 1.6 \text{ cm}^3 \text{ mol}^{-1}$ from the X-ray diffraction results of Ref. 7, which leads to a calculated initial slope of $\approx 6.6 \text{ deg kbar}^{-1}$, in serious disagreement with the present experimental results. It is difficult to imagine how the experimental slope could be too high by some 5 deg kbar^{-1} and, since the entropy change has been corroborated, the data

for the change in volume must be considered further. In particular, the anomalously rapid increase in volume⁷⁾ of low-CsSCN with temperature is suspect because the entropy change at the transition is large enough to include all of the orientational entropy due to end-for-end disordering of the $(\text{SCN})^-$ ion. It seems entirely possible that very little of the disordering takes place below the transition temperature and thus an obvious reason for the anomalous volume variation is eliminated. The high-low CsSCN transition is structurally dissimilar to the transitions in the other thiocyanates (which do show variations below the transition temperatures presumably due to progressive disordering) and it also shows hysteresis between transition temperatures on heating and cooling (in Fig. 2 of Ref. 7 and in Pacey's work, if not in the high pressure runs), unlike the other thiocyanate transitions. Correspondence with the senior author of Ref. 7 could not elicit any comment about the suspicions concerning the X-ray diffraction data on low-CsSCN at high temperatures.

Previously, the solid-solid transition in KSCN was discussed³⁾ entirely as a λ -transition, without any first-order component, *i.e.*, discontinuous volume or entropy change. This model³⁾, however, is inadequate because it cannot account for the experimental value of dT_1/dp —which they³⁾ did not consider at all. Appendix A discusses the thermodynamics of the high-low KSCN transition in a way more nearly in accord with the high pressure data and it is concluded that the transition is mostly λ -like, although with a small first-order component.

Since the structures of the low-KSCN, NH_4SCN , RbSCN and TlSCN phases apparently are isomorphous, it may be assumed that the structures of the high phases are also isomorphous and also that the transitions are similar thermodynamically. Pistorius' data (Appendix B) show that the lattice parameters for low- RbSCN and also low- NH_4SCN vary rapidly with temperature upon approaching the transitions, akin to the analogous data³⁾ for KSCN; it is not unlikely that TlSCN shows similar behavior. If the estimates for transition entropies and the observed slopes are combined *via* the Clausius-Clapeyron equation to estimate the corresponding volume changes at the transitions in RbSCN and NH_4SCN , it is clear that these volume changes are larger than those which might be deduced by extrapolation of Pistorius' data (Appendix B). Hence, it is suggested that the transition entropies observed by DSC for RbSCN and NH_4SCN include both isothermal and nonisothermal contributions, as for KSCN. More painstaking calorimetric and volumetric determinations will be necessary to establish the variations below and near the high-low transitions for these substances.

Even more careful calorimetry is unlikely, however, to alter the present observation that, despite the uncertainties as to how to subtract the background, the transition entropies vary progressively as 1.30 ± 0.05 ,²⁾ ≥ 0.6 , ≥ 0.3 , and $\geq 0.3 \text{ cal mol}^{-1} \text{ deg}^{-1}$ for KSCN, RbSCN , NH_4SCN , and TlSCN , respectively. On one hand, this progression could be used to argue against

the similarity of the transitions whilst, on the other hand, it could be used in an argument against the applicability of the molecular field model.³⁾ Taking the latter point of view, it is possible that the alternate formulation of Appendix A might be applicable but this is not demonstrable here for lack of necessary data.

It may be observed that the transition entropies decrease in order of increasing cation polarizability and that a similar progression has been recognized¹¹⁾ for the discontinuous entropy changes attending the isostructural transitions in K_2SO_4 , Rb_2SO_4 , Cs_2SO_4 , and Tl_2SO_4 . For these sulfates, it is arguable that much of the disordering takes place gradually below the transition and this is especially well demonstrated by the enthalpy data¹²⁾ for Tl_2SO_4 as compared to K_2SO_4 . The details of the disordering behavior in a sequence of isostructural compounds could be more conveniently investigated for these thiocyanates than for the sulfates because the temperatures are lower and the disordering more simply envisioned.

In the absence of data for microscopic order parameters, some consideration can be given to possible order parameters using available data and which can be devised from experience on transitions in other sequences of compounds. Thus, for instance, some M_2CO_3 transitions monoclinic \rightarrow hexagonal with increasing temperature-proved describable¹³⁾ with the order parameter [monoclinic angle -90°], which became rigorously zero above the transition temperatures; it was also possible¹³⁾ to scale the order parameters onto the same curve *vs.* 'reduced temperature' T/T_1 . On heating to the transition temperature, the greatest thermal expansions are in the direction perpendicular to the planar carbonate ion and this also occurs for NaNO_3 , AgNO_3 , CaCO_3 , *etc.* which have planar ions and λ -transitions. Likewise, for KSCN, NH_4SCN , RbSCN , and presumably TlSCN , the thermal expansion upon approaching the transition is greatest in the *c*-direction, which is perpendicular to the plane in which the $(\text{SCN})^-$ ions are disordering end-for-end.^{2,3)} Also, it may be verified that the thermal expansions in the *a*-, *b*-, and *c*-directions for the orthorhombic phases are linked to one another by plotting the lattice parameters, at the same temperature, for each pair and observing that straight lines are obtained, within the precision of the data and independent of the uncertainty in temperature. As a possible order parameter for the thiocyanate transitions, one may consider $[a-b]$ since this decreases monotonically with increasing temperature and is rigorously zero above the transition temperature. Comparing the KSCN and RbSCN data which are the most extensive, $[a-b]$ *vs.* T/T_1 show different courses and this can be attributed to the different temperature dependences of the anion disordering, as postulated above.

An important generalization concerning the polymorphism in some structurally similar sequences of substances has emerged from the accumulating data¹⁴⁾ on phase transitions at high pressures. To wit, the larger the ionic radius of the cation the lower the pressure at which structurally identical polymorphs are

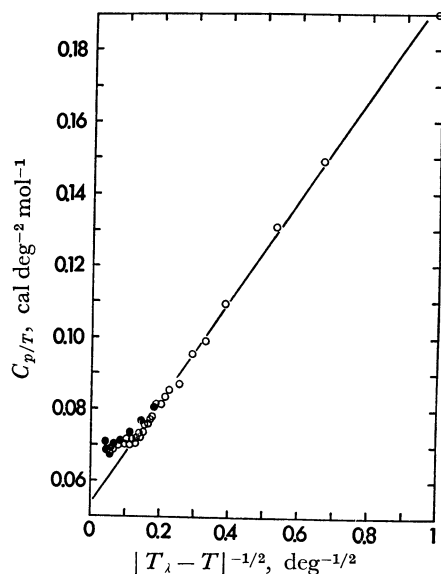


Fig. 5. Plots of $C_{p/T}$ vs. $(T_\lambda - T)^{-1/2}$ (open circles, for $T < T_\lambda$) and vs. $(1/4)(T - T_\lambda)^{-1/2}$ (filled circles, for $T > T_\lambda$) for KSCN.

encountered—and the validity of this empirical rule is surprisingly extensive.¹⁴ Nevertheless, the lack of any new polymorphs in the present investigation of NH_4SCN , RbSCN , and TlSCN , compared with the several high pressure polymorphs of KSCN ,¹ means that this empirical generalization is invalid for these thiocyanates.

Thanks are due to: the late C. W. F. T. Pistorius, P. W. Richter and J. B. Clark for encouragement and assistance; S. J. Pretorius and R. A. Pacey for the DSC and DTA-DSC runs. Much of the thinking about the KSCN transition was done whilst a Guggenheim Fellow at the Australian National University, Canberra, A. C. T.

Appendix A: Thermodynamics of the λ -like transition in KSCN

Yamada and Watanabe³ have given a description of the KSCN transition in terms of a molecular-field model with a volume-dependent interaction energy. Unfortunately they did not consider that the initial variation of transition temperature with pressure, dT_λ/dp , was an important constraint on their correlations and it does not appear that their model is consistent with the experimental value^{1,9} for $dT_\lambda/dp = 18.2 \pm 1.1$ deg kbar⁻¹. Here, the approach is more macroscopic and is along the lines of the discussion¹⁵ of the nematic-isotropic transition in *p*-azoxyanisole, which has a small first-order transition superimposed on a λ -like transition.

The heat capacity data² for KSCN are represented (Fig. 5) as

$$C_{p/T} = (C_{p/T})_0 + A|T_\lambda - T|^{-1/2}, \quad (\text{A-1})$$

where $(C_{p/T})_0 \approx 0.054$ cal deg⁻² mol⁻¹ and $A \approx 0.14$ cal deg^{-3/2} mol⁻¹ for $T < T_\lambda$ and about a quarter of this for $T > T_\lambda$. As shown in Fig. 5, Eq. A-1 is valid down to $(T_\lambda - T)^{-1/2} \approx 0.10$ or $T \approx T_\lambda - 100$ °C and up to $1/4(T - T_\lambda)^{-1/2} \approx 0.1$ or $T \approx T_\lambda + 6$ °C. Within this temperature range and using $T_\lambda = 139.2_0$ °C², only the tabulated data² for 139.27 °C and 139.52 °C deviate much from Eq. A-1 and the accuracy

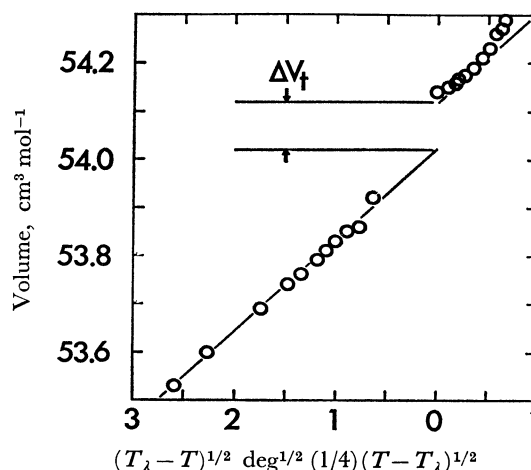


Fig. 6. Plot of molar volumes, for KSCN, vs. $(T_\lambda - T)^{1/2}$ for $T < T_\lambda$ and vs. $(1/4)(T - T_\lambda)^{1/2}$ for $T > T_\lambda$. The postulated volume discontinuity, ΔV_t , is indicated.

of these data very close to T_λ may be difficult to assess. The variation of thermal expansion with temperature may be anticipated from the Pippard relation¹⁵⁻¹⁷ involving $C_{p/T}$, $(\partial V/\partial T)_p$ and dT_λ/dp . Thus plots of the thermal expansion data^{3,18} vs. $|T_\lambda - T|^{-1/2}$ yield roughly linear fits over about the same temperature range for which Eq. A-1 is valid. Here, however, it is more accurate to describe the variation with temperature of the volumes—which were actually measured,^{3,18} the thermal expansions being derived therefrom—and Fig. 6 shows the molar volumes¹⁸ plotted vs. $(T_\lambda - T)^{1/2}$ for $T < T_\lambda$ and vs. $1/4(T - T_\lambda)^{1/2}$ for $T > T_\lambda$. For $T_\lambda = 142.7$ °C¹⁸ the slopes of the drawn lines (Fig. 6) are ≈ 0.19 cm³ deg^{-1/2} mol⁻¹, both above and below T_λ . It is inferred (Fig. 2) that there is a small, discontinuous volume change of ≈ 0.10 cm³ mol⁻¹ at the transition. Yamada and Watanabe³ chose not to identify a discontinuous volume change there whereas Plester *et al.*¹⁹ suggested a discontinuity of ~ 0.2 cm³ mol⁻¹, almost certainly an overestimate due to inadequate data for the rapid variations near T_λ .

The Pippard relation together with the value of A (Eq. A-1) and the slope of the plot in Fig. 6 suggest $dT_\lambda/dp \sim 16.3$ deg kbar⁻¹, which compares well with the experimental values.^{1,9} For the first-order component of the transition, the Clausius-Clapeyron equation suggests a discontinuous entropy change of ~ 0.14 cal deg⁻¹ mol⁻¹ and this may be within the uncertainties in the heat capacity data² near T_λ .

Appendix B: Lattice parameters of RbSCN and NH_4SCN at high temperatures

by C. W. F. T. PISTORIUS

Diffraction scans were made of RbSCN and NH_4SCN from the same stocks as used elsewhere in this paper. High temperature work was done with an MRC X-86-N attachment. For RbSCN at 23 °C, 54 reflections, up to (164), were observed and were consistent with Pbcm—as for KSCN ²⁰ and TlSCN ²¹ below the solid-solid transition; the lattice parameters thus obtained were $a = 6.842$, $b = 6.895$, and $c = 8.019$ Å. For RbSCN at high temperatures, the following reflections were observed — (020), (200), (112), (022), (202), (122), (212), (130), (310), (224), (412)—and, above the transition, (112), (202), (220), (130), (224), (312). The lattice parameters deduced from these observed reflections are listed in Table B1, perhaps accurate to $\pm 0.1\%$, at the various temperatures, accurate

TABLE B1. LATTICE PARAMETERS OF RbSCN AND NH₄SCN AT HIGH TEMPERATURES

$T(^{\circ}\text{C})$	$a(\text{\AA})$	$b(\text{\AA})$	$c(\text{\AA})$	$\beta(\text{deg})$
RbSCN				
23	6.842	6.896	8.017	
55	6.851	6.903	8.042	
75	6.856	6.909	8.060	
100	6.864	6.915	8.089	
120	6.872	6.922	8.114	
140	6.883	6.929	8.146	
161	6.901	6.938	8.179	
162		6.945	8.245	
180		6.948	8.264	
NH ₄ SCN				
22	4.247 \pm 3	7.146 \pm 5	13.022 \pm 8	97.8 ₇
84	4.285 \pm 5	7.180 \pm 7	12.973 \pm 12	98.1 ₇
88. ₅	6.874 \pm 6	6.903 \pm 6	7.878 \pm 8	
102. ₅	6.878 \pm 4	6.905 \pm 4	7.912 \pm 6	
117. ₅	6.898 \pm 6	6.912 \pm 6	7.954 \pm 8	
140. ₅		6.961 \pm 6	8.000 \pm 8	

to $\pm 5^{\circ}\text{C}$. For NH₄SCN, lattice parameters were deduced from the (013), (102), (022), (112), (11 $\bar{3}$), (121), (113), (12 $\bar{2}$), and (015) reflections for the monoclinic phase, from the (121), (331), (042), (402), and several other reflections (all compatible with Pbcm) for the orthorhombic phase and from the (210), (112), (121), and (020) reflections for the tetragonal phase; the results are listed in Table B1, at the various temperatures, accurate to $\pm 5^{\circ}\text{C}$ above room temperature.

References

- 1) C. W. F. T. Pistorius, J. B. Clark, and E. Rapoport, *J. Chem. Phys.*, **48**, 5123 (1968).
- 2) M. Sakiyama, H. Suga, and S. Seki, *Bull. Chem. Soc. Jpn.*, **36**, 1025 (1963).
- 3) Y. Yamada and T. Watanabé, *Bull. Chem. Soc. Jpn.*, **36**, 1032 (1963).
- 4) C. W. F. T. Pistorius and J. C. A. Boeyens, *J. Chem. Phys.*, **48**, 1018 (1968).
- 5) Powder diffraction file-card No. 23—29.
- 6) I. Lindquist, *Acta Crystallogr.*, **10**, 29 (1957).
- 7) S. Manolatos, M. Tillinger, and B. Post, *J. Solid State Chem.*, **7**, 31 (1973).
- 8) C. W. F. T. Pistorius and J. B. Clark, *High Temp. High Press.*, **1**, 561 (1969); P. W. Richter and C. W. F. T. Pistorius, *J. Solid State Chem.*, **3**, 197 (1971).
- 9) P. W. Bridgman, *Proc. Am. Acad. Arts Sci.*, **51**, 55 (1915).
- 10) J. B. Wrzesnewsky, *Z. Anorg. Chem.*, **74**, 95 (1912).
- 11) H. F. Fischmeister, *Z. Phys. Chem. Neue Folge*, **7**, 91 (1959).
- 12) A. S. Dworkin and M. A. Bredig, *J. Phys. Chem.*, **74**, 3403 (1970).
- 13) W. Klement and L. H. Cohen, *Ber. Bunsenges. Phys. Chem.*, **79**, 327 (1975).
- 14) C. W. F. T. Pistorius, *Prog. Solid State Chem.*, in press.
- 15) W. Klement and L. H. Cohen, *Mol. Cryst. Liq. Cryst.*, **27**, 359 (1974).
- 16) A. B. Pippard, *Phil. Mag.*, **1**, 473 (1956).
- 17) W. Klement, *J. Phys. Chem.*, **74**, 2753 (1970).
- 18) T. Shinoda, H. Suga, and S. Seki, *Bull. Chem. Soc. Jpn.*, **33**, 1314 (1960).
- 19) D. W. Plester, S. E. Rogers, and A. R. Ubbelohde, *Proc. Roy. Soc. (London)*, **A235**, 469 (1956).
- 20) Powder diffraction file-card No. 9—388.
- 21) Powder diffraction file-card No. 8—65.